Copyright © 2004 Tech Science Press CMES, vol.5, no.1, pp.73-80, 2004

Analysis of Densification and Swelling of Solids Using Pressure Dependent Plasticity Criteria

J. Larsson[1], J. Faleskog[1] and A.R. Massih[2 3]

Abstract: We consider certain constitutive laws for analyzing the elastic-plastic behavior of granular material, which is subjected to compressive hydrostatic stresses and concomitantly undergoing swelling. The plastic yield functions for this kind of materials are pressure and porosity dependent. The constitutive laws are formulated in a finite element (FE) framework for applications to structures involving granular/porous materials. We have employed an implicit and unconditionally stable algorithm for numerical integration of the constitutive relations. The numerical method has been programmed in a FE computer code. The code is then used to study a plane strain problem for a range of model parameters and yield criteria, where the stress response of material under compressive loads is evaluated. Finally the method is applied to the case of B_4C powder encased in a stainless steel tube, which is subjected to compressive loads under swelling condition.

keyword: Densification, swelling, pressure dependent plasticity, FEM.

1 Introduction

Granular materials are utilized in many industrial products and processes. They have peculiar and complex mechanical properties, understanding of which is important for the design and performance of these products. In this paper we use certain constitutive laws for analyzing the elastic-plastic behavior of granular material, which is subjected to compressive hydrostatic stresses and concomitantly undergoing swelling. The main plastic yield criterion considered here is a "regularized" variant of the Drucker-Prager model [Drucker and Prager (1952)], which was proposed some years ago by Kuhn and Downey (1971) and independently by Green (1972). The Kuhn-Downey-Green (KDG) model assumes that the yield criterion is a function of the first invariant of the deviator stress, σ_I, and the second invariant of the deviator stress, s_{II}, i.e., $F = F(s_{II}, \alpha\sigma_I, \beta\kappa)$ where α and β are functions of the relative density (or porosity) and κ is the yield stress. Shima and Oyane (1976) determined the density dependence of α and β by means of uniaxial compression tests for copper powders with initial relative densities ranging from 0.62 to 0.87. We have employed similar functional forms for α and β as described in [Shima and Oyane (1976)].

We also regard, for the sake of comparison, the Gurson yield criterion [Gurson (1977)], which in its original form describes a porous solid consisting of a rigid perfectly plastic matrix containing spherical cavities of equal size. The Gurson model, which provides a mechanistic description of deformation of porous solid, is appropriate for low porosities [Redanz (1997)], (best for relative densities greater than 0.90.)

The basic characteristic of these models is that the yield functions give ellipsoidal yield surfaces in stress space and are symmetric with respect to hydrostatic tension and compression. Moreover, the functions are isotropic with the material response expressed in terms of a single state variable, the porosity. When porosity vanishes, these yield functions reduce to the von Mises yield criterion used in metal plasticity, i.e. the yield function forms a cylindrical surface in stress space. The stress-strain $\sigma - \varepsilon$ constitutive relations, in incremental form, are $d\varepsilon = d\gamma(\partial F/\partial\sigma)$, where $d\gamma$ is a non-negative constant. We will utilize these models with the consideration that the material porosity changes during the deformation process.

There are other mechanistic models of powder compaction, e.g., Helle, Easterling, and Ashby (1985) and Fleck (1995). These models, as for the Gurson model, are usually valid in a narrow range of relative density. Also, they contain material-dependent parameters, which

[1] Royal Institute of Technology, SE-100 44 Stockholm, Sweden
[2] Malmö University, SE-205 06 Malmö, Sweden
[3] Quantum Technologies AB, SE-751 83 Uppsala, Sweden

need to be determined experimentally.

In this paper the aforementioned constitutive laws (KDG and Gurson) are formulated in a finite element (FE) framework for applications to structures involving granular/porous materials. We have employed an implicit and unconditionally stable algorithm, based on the work of Aravas (1987) and Govindarajan and Aravas (1995), for numerical integration of the elastoplastic constitutive relations. The numerical method has been programmed in the user-defined module of the FE computer code ADINA (1999). The code is then used to study a plane strain problem for a range of model parameters and the two yield criteria, where the stress response of material under compressive loads is evaluated. Finally the method is applied to the case of B_4C powder encased in a stainless steel tube, which is subjected to compressive loads under swelling condition. The present study is a continuation of our preceding works [Massih, Isaksson, and Ståhle (1997), Massih (2000)] on plasticity of granular material, where the case of perfect plasticity (constant pore volume) was analyzed.

2 Plasticity criteria

We first consider the Kuhn-Downey-Green criterion [2,3] for plasticity of porous solids. The yield stress function for this criterion is expressed as

$$F = q^2/\kappa^2 + 9\alpha p^2/\kappa^2 - \beta \leq 0, \tag{1}$$

where $q = \sqrt{3 s_{II}}$, $p = -\sigma_I/3$, $s_{II} = \mathrm{tr}(s^2)/2$, $\sigma_I = \mathrm{tr}(\sigma)$, and $s = \sigma - \mathrm{tr}(\sigma)1/3$. Here σ is the stress tensor, 1 is the second order unit tensor, α, β are positive scalar parameters depending on the material density (or porosity) and κ is the yield stress of the solid matrix. The relative density of the body ρ is related to the porosity fraction f via $\rho = f - 1$. We select the following form:

$$\alpha = a f^m; \quad \beta = (1-f)^{2n}, \tag{2}$$

where a, m and n are material dependent parameters, identified from measurements.

The other pressure-dependent yield criterion considered here is the Gurson model [Gurson (1977)], described as

$$F = q^2/\kappa^2 + 2k_1 f \cosh(\frac{3k_2 p}{2\kappa}) - (1 + k_1^2 f^2) \leq 0, \tag{3}$$

where the adjusting parameters k_1 and k_2 were introduced by Tvergaard (1982) to account for void interaction effects, which is of special interest in situations where pore concentration is significant.

Using an associated flow rule the plastic strain rate is derivable from the yield function $F = F(p,q)$, in the form

$$\dot{\varepsilon}^p \equiv \dot{\gamma}\frac{\partial F}{\partial \sigma} = \dot{\gamma}(\frac{\partial F}{\partial p}\frac{\partial p}{\partial \sigma} + \frac{\partial F}{\partial q}\frac{\partial q}{\partial \sigma}), \tag{4}$$

where $\dot{\gamma}$ is the plastic rate multiplier, and an overdot indicates differentiation with respect to time t. Equation (4) can be reduced to

$$\dot{\varepsilon}^p = \frac{1}{3}\dot{P}1 + \dot{Q}n, \tag{5}$$

where $\dot{P} \equiv -\dot{\gamma}\,\partial F/\partial p$, $\dot{Q} \equiv \dot{\gamma}\,\partial F/\partial q$, $\partial p/\partial \sigma = -1/3$ and $\partial q/\partial \sigma = 3s/2q \equiv n$. Furthermore, the Cauchy stress tensor can be expressed in the manner

$$\sigma = -p1 + \frac{2}{3}q\,n. \tag{6}$$

For the two yield criteria considered here, i.e. relations (1) and (3), we assume the following time evolution law for material porosity fraction (void volume fraction):

$$\dot{f} = (1-f)\mathrm{tr}(\dot{\varepsilon}^p) = (1-f)\dot{P}. \tag{7}$$

The total strain rate tensor for the material is the sum of three contributions, elastic, plastic and swelling, where the densification strain rate is included in the plastic term. We write:

$$\dot{\varepsilon} = \dot{\varepsilon}^e + \dot{\varepsilon}^p + \dot{\varepsilon}^s, \tag{8}$$

where in our case $\dot{\varepsilon}^s = \Phi =$ constant and Φ, the swelling rate, is identified from measurement. We should mention

that for the problem under consideration $\dot{f} < 0$, meaning that porosity decreases under compression.

Assuming linear elasticity, Hooke's law gives

$$\sigma = C^e : \varepsilon^e \Leftrightarrow \sigma_{ij} = C^e_{ijkl}\varepsilon^e_{kl}, \tag{9}$$

where C^e is the fourth-order elasticity tensor. For isotropic elasticity, this tensor is described according to relation: $C^e = \lambda 1 \otimes 1 + 2\mu I$, where I is the fourth-order symmetric unit tensor and λ and μ are the Lamé constants, related to Young's modulus E and Poisson's ratio ν.

The plastic rate multiplier can be found from the consistency condition $\dot{F} = (\partial F/\partial q)\dot{q} + (\partial F/\partial p)\dot{p} = 0$ which after some algebra yields

$$\dot{\gamma} = \frac{-(\partial F/\partial p)\mathrm{tr}(\dot{\varepsilon}) + 2\zeta(\partial F/\partial q)\mathrm{tr}(\dot{e}n)}{(\partial F/\partial p)^2 + 3\zeta(\partial F/\partial q)^2}, \tag{10}$$

where $\zeta = 3(1-2\nu)/2(1+\nu)$ and $\dot{e} = \dot{\varepsilon} - \mathrm{tr}(\dot{\varepsilon})1/3$ is the deviatoric strain rate tensor.

3 Numerical integration and linearization

In the framework of finite element method the constitutive relations are evaluated at the element integration points. During the computation process the total strain is known and the individual strains (the right hand side of relation (8)) and the state variables (material porosity in our case) are updated. The elasticity relations (9) give:

$$\sigma_{t+\Delta t} = C^e : \varepsilon^p_{t+\Delta t} = \sigma^e - C^e : \Delta\varepsilon^p, \tag{11}$$

where $\sigma^e = C^e : (\varepsilon^e_t + \Delta\varepsilon)$ is the elastic trial stress tensor, $\Delta\varepsilon$ is the increment of the total strain tensor and Δt is the time increment. For the present calculation we have adopted the Euler backward scheme presented by Aravas (1987). In this scheme the plastic strain increment $\Delta\varepsilon^p$ is expressed as:

$$\Delta\varepsilon^p = \frac{1}{3}\mathfrak{p}1 + \mathfrak{q}n_{t+\Delta t}, \tag{12}$$

where $\mathfrak{p} \equiv -\Delta\gamma(\partial F/\partial p)_{t+\Delta t}$, $\mathfrak{q} \equiv \Delta\gamma(\partial F/\partial q)_{t+\Delta t}$ and $\Delta\gamma$ is the increment of the plastic multiplier. Also equation (6) can be rewritten as:

$$\sigma_{t+\Delta t} = -p_{t+\Delta t}1 + \frac{2}{3}q_{t+\Delta t}\, n_{t+\Delta t}. \tag{13}$$

Invoking the relation for C^e and using equation (12) we can express equation (11) in the form

$$\sigma_{t+\Delta t} = \sigma^e - (\lambda + \frac{2}{3}\mu)\mathfrak{p}1 - 2\mu\mathfrak{q}n_{t+\Delta t}. \tag{14}$$

We note that equation (14) gives: $s_{t+\Delta t} = s^e - 2\mu\mathfrak{q}n_{t+\Delta t}$, where s^e is the deviatoric stress corresponding to σ^e. Therefore, in the deviatoric stress space, the return to the yield surface is along $n_{t+\Delta t}$, implying that s^e is coaxial with $s_{t+\Delta t}$ and hence can directly be found from σ^e via the relation: $n_{t+\Delta t} = (3/2q^e)s^e$, where $q^e = \sqrt{3\mathrm{tr}(s^e s^e)/2}$.

The primary unknowns in equation (14), $\mathfrak{p}$ and $\mathfrak{q}$, are found by using the equations collected in Box 3.1, where $F_{t+\Delta t} \equiv F(p_{t+\Delta t}, q_{t+\Delta t}, f_{t+\Delta t})$ and $K = \lambda + 2\mu/3$ is the modulus of elasticity. This set of equations are solved by Newton's method in the user-defined subroutine of the ADINA program, ADINA (1999).

$$\begin{aligned}
\mathfrak{p}(\partial F/\partial q)_{t+\Delta t} &= -\mathfrak{q}(\partial F/\partial p)_{t+\Delta t} && (15)\\
p_{t+\Delta t} &= p^e_{t+\Delta t} + K\mathfrak{p} && (16)\\
q_{t+\Delta t} &= q^e_{t+\Delta t} - 3\mu\mathfrak{q} && (17)\\
f_{t+\Delta t} &= (f_t + \mathfrak{p})(1+\mathfrak{p})^{-1} && (18)\\
F_{t+\Delta t} &= 0 && (19)
\end{aligned}$$

Box 3.1: Relations for finding $\mathfrak{p}$ and $\mathfrak{q}$.

The consistent tangent modulus, for the backward Euler update method, is calculated as $C^a = (\partial\sigma/\partial\varepsilon)_{t+\Delta t}$. Using equation (14), and omitting the subscript $t+\Delta t$, we find

$$\frac{\partial\sigma}{\partial\varepsilon} = K\Big(1 - \frac{\partial\mathfrak{p}}{\partial\varepsilon}\Big)\otimes 1 + 2\mu\Big(\frac{\partial e}{\partial\varepsilon} - \frac{\partial(\mathfrak{q}n)}{\partial\varepsilon}\Big), \tag{20}$$

where $\partial(\mathfrak{q}n)/\partial\varepsilon = (\partial\mathfrak{q}/\partial\varepsilon)\otimes n + \mathfrak{q}(\partial n/\partial\varepsilon)$.

The explicit expressions for the terms appearing in the tangent modulus (20) can be derived for computation fol-

lowing the work of Govindarajan and Aravas (1995). In our notation, the differentials of the state variables, obtained from relations (16)-(18), are expressed as:

$$dp = -K\Big(\mathrm{tr}(d\varepsilon) - d\mathfrak{p}\Big), \tag{21}$$

$$dq = \mu\Big(2n : d\varepsilon - 3d\mathfrak{q}\Big), \tag{22}$$

$$df = (1-f)(1+\mathfrak{p})^{-1} d\mathfrak{p}. \tag{23}$$

Taking the total differential of relation (16) and substituting for dp, dq and df from equations (21)-(22), we obtain the following matrix relation:

$$[A]\{\frac{\partial \mathfrak{p}}{\partial \varepsilon}, \frac{\partial \mathfrak{q}}{\partial \varepsilon}\} = [B]\{1, n\}, \tag{24}$$

where $[A]$ and $[B]$ are 2×2 matrices with components A_{ij} and B_{ij}, respectively. The brace symbol in equation (24) denotes a column vector with two components. Equation (24) can formally be solved for $\partial\mathfrak{p}/\partial\varepsilon$ and $\partial\mathfrak{q}/\partial\varepsilon$ according to:

$$\{\frac{\partial \mathfrak{p}}{\partial \varepsilon}, \frac{\partial \mathfrak{q}}{\partial \varepsilon}\} = [M]\{1, n\}, \tag{25}$$

where $[M] = [A^{-1}][B]$. The components of the matrix $[M]$, for the problem under consideration, are listed in the appendix. Hence the tangent modulus is expressed as the sum of a symmetric and an unsymmetric fourth-order tensor:

$$\frac{\partial \sigma}{\partial \varepsilon} = A_{sym} + B_{uns} \tag{26}$$

where

$$A_{sym} = 2\mu\Big(\frac{q}{q^e} J + N_{22} n\otimes n\Big) + K(1-M_{11}) 1\otimes 1, \tag{27}$$

$$B_{uns} = -2\mu M_{21} n\otimes 1 - K M_{12} 1\otimes n, \tag{28}$$

$N_{22} = (2/3)(1-q/q^e) - M_{22}$ and $J = I - 1\otimes 1/3$. Note that B_{uns} becomes symmetric when $M_{12} = 2\mu M_{21}/K$. On the other hand, comparing the M-matrix components given in the appendix, we find

$$M_{12} = \frac{2\mu}{K}\frac{M_{21}}{1+\chi\mathfrak{q}}, \tag{29}$$

where χ is defined in the appendix. As has been noted by Aravas (1987), the use of unsymmetric stiffness matrix in a finite element program slows down the rate of convergence of the Newton iterations of the equilibrium equation. However, in our case $\mathfrak{q}$ is of the order of 0.01 or less, hence the lack of symmetry should not degrade the rate of convergence appreciably, if the unsymmetrical part of the tangent modulus is symmetrized.

4 Example: A plate subjected to compression under swelling

Let us apply the foregoing method to a square plate with side length L fixed at three sides and subjected to a compressible displacement from one side (plane strain condition). Our aim is to study the influence of model parameters on the plastic response of the material. We consider the KDG yield criterion with material property data listed in Tab. 1 and the Gurson criterion for two sets of adjusting parameters, the original Gurson values $k_1 = 1$, $k_2 = 1$ and the Tvergaard (1982) values, $k_1 = 1.5$, $k_2 = 1$, for $f_0 = 0.3$. Furthermore, we impose a swelling rate $\Phi = 2.59\times 10^{-6}\ \mathrm{h}^{-1}$ and a compressive strain rate $\dot{w} = 3.60\times 10^{-6}\ \mathrm{h}^{-1}$ in the material.

Table 1 : Material property data used in plate example.

KDG parameter	Case I	Case II
a	0.698	1.1
m	1.08	1.1
n	2.5	0.0
$E = 191$ GPa	$\nu = 0.18$	$\kappa = 300$ MPa

The results of our FE analysis using the KDG criterion are depicted in Fig. 1, where the equivalent stress is plotted against time for the two considered cases. We notice that in case I, right after plastic yielding, the equivalent stress exhibits a softening effect, whereas in case II a hardening behavior is observed. The change from softening to hardening occurred when $a \approx 1$. This behavior was not witnessed when we employed the Gurson criterion with the two sets of aforementioned coefficients,

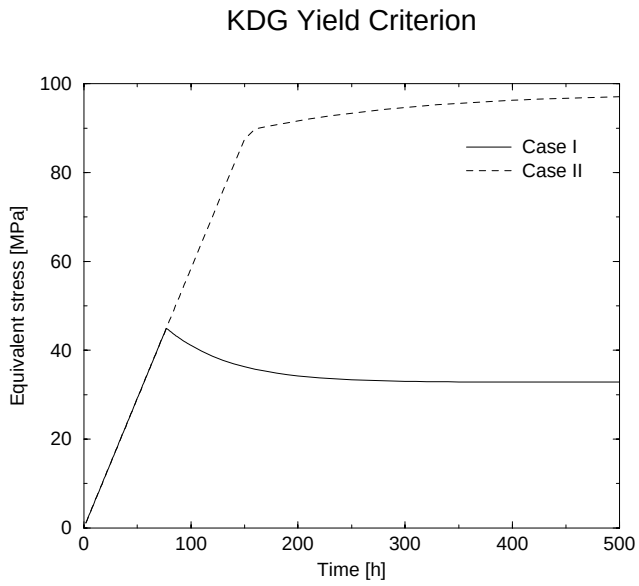

Figure 1 : The equivalent stress in the plate versus time under plane strain condition. The KDG criterion, for the two cases listed in Tab. 1, is used in the computations.

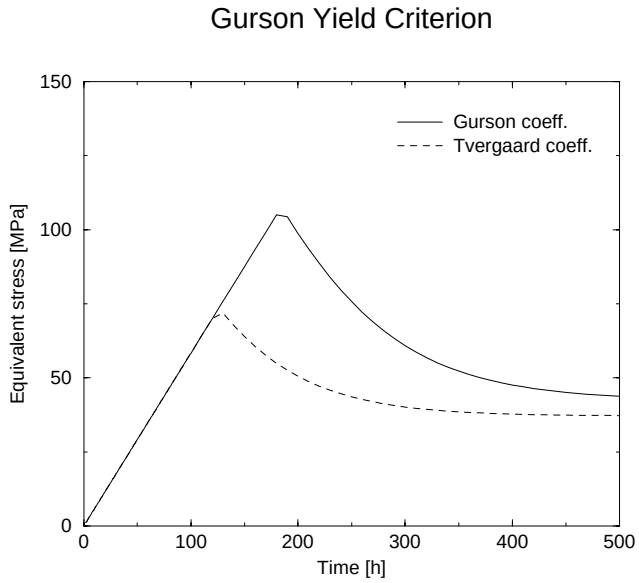

Figure 2 : The equivalent stress in the plate versus time under plane strain condition. The Gurson criterion for the two sets of adjusting coefficients is used in the computations.

Fig. 2.

We have also checked the accuracy of our finite element method by comparing the results of calculations on case I for p versus q with direct numerical solution (Euler's method) of the exact analytical relations derived for the plate, Larsson (2001). The match between the results of the two methods is practically complete for time steps below $\Delta t = 100$ h.

5 Application: boron carbide powder in a steel tube

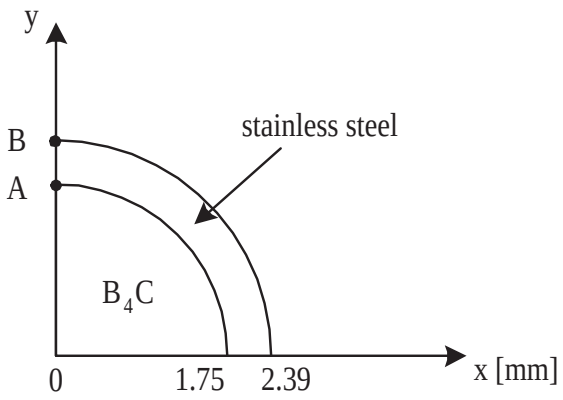

Figure 3 : A quarter of tube geometry that is modeled.

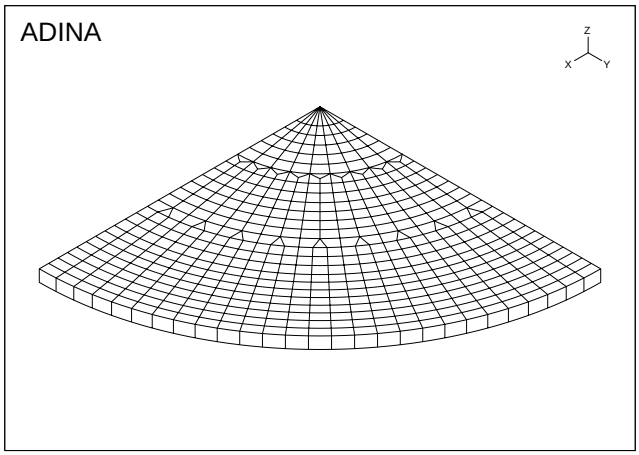

Figure 4 : The finite element mesh used in the analysis.

We consider an example from nuclear engineering, i.e. the case of a control rod of a boiling water reactor consisting of B_4C powder (neutron absorber) encased in a stainless steel tube, Fig. 3. Three-dimensional isoparametric 20-node solid element of the ADINA program is

used for the structure with a mesh shown in Fig. 4. Generalized plane strain condition and perfect contact (no sliding) between B_4C and steel are assumed.

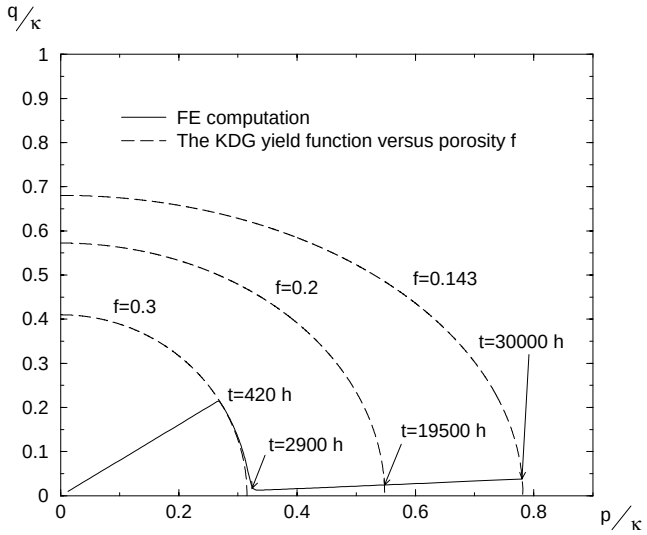

Figure 5 : B_4C powder confined in a steel tube subjected to compressible hydrostatic pressure. The solid curve shows the evolution of the equivalent stress q versus the hydrostatic pressure p during densification. Here κ is the flow stress of the material and f the porosity fraction.

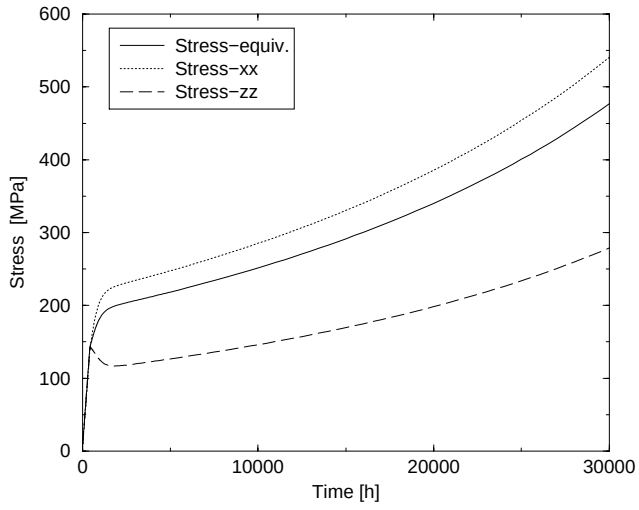

Figure 6 : Stresses at the outer rim of the tube (element B, Fig. 3) versus time. `Stress-equiv.` is the von Mises equivalent stress.

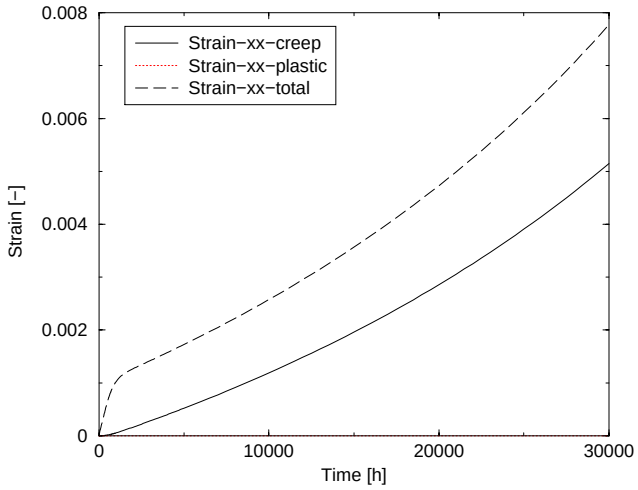

Figure 7 : Strains at the outer rim of the tube (element B, Fig. 3) versus time. The plastic strain component is nil.

During reactor service, B_4C swells and is subjected to mechanical interaction with the tube. We suppose that B_4C obeys the KDG yield criterion, with material properties listed for case I in Tab. 1, and the swelling rate of $\Phi = 2.59 \times 10^{-6}\ \mathrm{h}^{-1}$. The stainless steel tube is assumed to obey the von Mises yield criterion, with $E =$ 175 GPa, $\nu = 0.3$, and the creep strain rate $\dot{\varepsilon}_{ss}^{creep} = 6.68 \times 10^{-10}\sigma_{eq}$, in unit of h^{-1}, where σ_{eq} is the equivalent von Mises stress in MPa at the service temperature of 300 °C.

By running the ADINA program the stresses and strains in the B_4C and in the tube wall are calculated as a function of time. In Fig. 5 we have depicted the evolution of the equivalent stress q versus the hydrostatic pressure p in B_4C (element A, Fig. 3) during densification and the evolution of the yield surface due to the decrease in porosity. We note that in the elastic regime, q increases with p till the yield surface is reached. Then on the yield surface, as time evolves, the stresses tend to hydrostatic pressure, rendering q to decrease until the porosity is reduced sufficiently leading to a slow raise in q. Fig. 6 shows the time evolution of the stresses at the outer surface of the tube (element B, Fig. 4). The total hoop strain is calculated to be about 0.8% after 30000 h of irradiation, Fig. 7. No time-independent plastic deformation of stainless steel tube was found, i.e. all the permanent deformation is due to irradiation creep according to our calculations.

5.1 Discussion

Post irradiation examinations made on boiling water control rods, consisting of B_4C powder with $f = 0.30$ encased in Type 304 stainless steel tube included measurements of tube diameter changes and the powder density, Fuhrman (1986). Measurements of tube diameter changes using mechanical profilometer showed a maximum permanent hoop strain of 0.2% over the top 0.51 m of the rod at end-of-life. The measurements of B_4C powder densities in this region by pycnometry of samples showed that B_4C particles swelled on average up to about 26% in volume. Our calculation shows that the permanent hoop strain of tube is around 0.5%, Fig. 7. The corresponding volumetric swelling correlation we used gives $\Delta V/V = 3\Phi t \approx 0.23$ at $t = 30000$ h. Hence with the material properties utilized, we over estimate the tube strain by a factor larger than 2. However, we attribute part of this over estimation to the choice of our irradiation-induced creep correlation for stainless steel, which has an upper-bound characteristic. If we choose a best-estimate type creep correlation, e.g. that of Foster, Wolfer, Biancheria, and Boltax (1972) we find $\dot{\varepsilon}_{ss}^{creep} \approx 2.78 \times 10^{-10}\sigma_{eq}$, i.e. a factor of $2.78/6.68 \approx 0.42$ lower than the used value.

Moreover, we should mention that long irradiation times in boiling water reactor core, cause embrittlement of the stainless steel material, due to the phenomenon of intergranular stress corrosion cracking, which eventually results in through wall cracks in the tube for strains larger than 0.2%, Fuhrman (1986). This type of evaluation takes us beyond the scope of the present paper.

Acknowledgement: We thank Tero Manngård for comments on the manuscript.

References

ADINA R and D Inc., Watertown, MA. *Theory and Modeling Guide Volume I: ADINA*, 1999.

Aravas, N. (1987): On the numerical integration of a class of pressure-dependent plasticity models. *International Journal of Numerical Methods in Engineering*, vol. 24, pp. 1395–1416.

Drucker, D. C.; Prager, W. (1952): Soil mechanics and plastic analysis or limit design. *Quarterly of Applied Mathematics*, vol. 10, pp. 157–165.

Fleck, N. (1995): On the cold compaction of powders. *Journal of the Mechanics and Physics of Solids*, vol. 43, pp. 1409–1431.

Foster, J.; Wolfer, W. G.; Biancheria, A.; Boltax, A. (1972): Analyses of irradiation induced creep of stainless steel in fast spectrum reactors. In *European Conference on Irradiation Embrittlement and Creep in Fuel Cladding*. British Nuclear Society.

Fuhrman, N. (1986): Behavior of irradiated B_4C. Technical Report NP-4533-LD, Electric Power Research Institute, Palo Alto, California, 1986.

Govindarajan, R. M.; Aravas, N. (1995): Pressure-dependent plasticity models: Loading-unloading criteria and the consistent linearization of an integration algorithm. *Communications in Numerical Methods in Engineering*, vol. 11, pp. 339–345.

Green, R. J. (1972): Plasticity theory of porous solids. *International Journal of Mechanical Science*, vol. 14, pp. 215–222.

Gurson, A. L. (1977): Continuum theory of ductile rupture by void nucleation and growth: Part 1 - yield criteria and flow rules for porous ductile media. *Journal of Engineering Materials & Technology*, vol. 19, pp. 2–15.

Helle, A.; Easterling, K.; Ashby, M. (1985): Hot-isostatic pressing diagrams: new developments. *Acta Metallurgica*, pp. 2163–2174.

Kuhn, H. A.; Downey, C. L. (1971): Deformation characteristic and plasticity theory of sintered powder materials. *International Journal of Powder Metallurgy*, vol. 7, pp. 15–25.

Larsson, J. (2001): Numerical implementation of pressure sensitive plasticity models. Master's thesis, Royal Institute of Technology, Stockholm, Sweden, 2001. In Swedish.

Massih, A. R. (2000): A plasticity model for swelling and densification of porous solids. In Atluri, S. N.; Burst, F. W.(Eds): *Advances in Computational Engineering and Sciences*, volume 1, pp. 452–257, Palmdale, CA. TECH Science Press.

Massih, A. R.; Isaksson, P.; Ståhle, P. (1997): Modeling the behavior of a control-element blade during irradiation. *Computers & Structure*, vol. 64, pp. 1113–1127.

Ngo, N. D.; Tamma, K. K. (2004): An Integration Comprehensive Approach to the Modeling of Resin

Transfer Molded Composite Manufactured Net-Shaped Parts, *CMES: Computer Modeling in Engineering & Sciences*, Vol. 5, No. 2, pp. 103-133.

Redanz, P. (1997): Numerical modelling of a cold compaction of metal powder. Technical Report 551, Technical University of Denmark, Lyngby, Denmark, 1997.

Shima, S.; Oyane, M. (1976): Plasticity theory for porous metals. *Interantional Journal of Mechanical Science*, vol. 18, pp. 285–291.

Tvergaard, V. (1982): On localization in ductile materials containing voids. *International Journal of Fracture Mechanics*, vol. 18, pp. 237–252.

Appendix A: Components of the M-matrix in relation (24)

Algebraic manipulations result in the following expressions for the components of the matrix $[M]$ defined through relation (25):

$$M_{11} = K(F_p^2 + 3\mu R_1)/D \quad (30)$$

$$M_{12} = -2\mu F_p F_q/D \quad (31)$$

$$M_{21} = -KF_p F_q(1+\chi\mathfrak{q})/D \quad (32)$$

$$M_{22} = 2\mu E/D \quad (33)$$

$$D = KF_p^2 + f_\mathfrak{p} F_f F_q + 3\mu E \quad (34)$$

$$E = F_q^2 + KR_1 + f_\mathfrak{p} R_2 \quad (35)$$

$$\chi = f_\mathfrak{p}(F_p F_{pf} - F_f F_{pp})/(F_p F_q) \quad (36)$$

$$R_1 = F_{pp} F_q \mathfrak{q} - F_{qq} F_p \mathfrak{p} \quad (37)$$

$$R_2 = F_{pf} F_q \mathfrak{q} - F_{qq} F_f \mathfrak{p} \quad (38)$$

where we have utilized the notation, $F_q = \partial F/\partial q$, $F_{pf} = \partial^2 F/\partial p \partial f$, etc. Also for the problem under consideration, $F_{pq} = F_{qp} = 0$. Comparing equation (31) with (32) we obtain equation (29) of the paper.